HHS Public Access

Author manuscript

J Immunol. Author manuscript; available in PMC 2024 May 15.

Published in final edited form as:

J Immunol. 2023 May 15; 210(10): 1519–1530. doi:10.4049/jimmunol.2200221.

The adjuvant combination of dmLT and MPL-A activates the canonical, non-pyroptotic NLRP3 inflammasome in dendritic cells and significantly interact to expand antigen-specific CD4 T cells

David L. Bauer[*], **Louay Bachnak**[*], **Vanessa M. Limbert**[*], **Rebecca M. Horowitz**[*], **Robin L. Baudier**[†], **Shaina J D'Souza**[*], **Victoria E. Immethun**[*], **Jonathan R Kurtz**[*], **Samuel B. Grant**[*], **James B. McLachlan**[*]

[*] Department of Microbiology and Immunology, Tulane University School of Medicine, New Orleans, LA, USA

[†] Department of Epidemiology, Tulane School of Public Health and Tropical Medicine, New Orleans, LA, USA

Abstract

Adjuvants are often essential additions to vaccines that enhance the activation of innate immune cells, leading to more potent and protective T and B cell responses. Only a few vaccine adjuvants are currently used in approved vaccine formulations in the US. Combinations of one or more adjuvants have the potential to increase the efficacy of existing and next generation vaccines. Here, we investigated how the non-toxic double mutant *Escherichia coli* heat labile toxin R192G/L211A (dmLT), when combined with the TLR4 agonist monophosphoryl lipid A (MPL-A), impacted innate and adaptive immune responses to vaccination in mice. We found that the combination of dmLT and MPL-A induced an expansion of antigen specific, multifaceted Th1/2/17 CD4 T cells higher than that explained by adding responses to either adjuvant alone. Furthermore, we observed more robust activation of primary mouse bone marrow derived dendritic cells in the combination adjuvant treated group via engagement of the canonical NLRP3 inflammasome complex. This was marked by a multiplicative increase in the secretion of active IL-1β that was independent of classical gasdermin D-mediated pyroptosis. Moreover, the combination adjuvant increased the production of the secondary messengers cAMP and prostaglandin E2 in dendritic cells. These results demonstrate how certain adjuvant combinations could be used to potentiate better vaccine responses to combat a variety of pathogens.

Corresponding author: James B McLachlan, Ph.D. Microbiology and Immunology, Tulane University School of Medicine, 1430 Tulane Ave. Room 5700, New Orleans, LA 70112, Phone: (504) 988-1626, Jmclachl@tulane.edu.

Author Contributions

Conceptualization: DLB, JRK, JBM
Methodology: DLB, JRK, RLB, JBM
Investigation: DLB, LB, VML, RMH, RLB, JRK, VEI, SJD, SG, JBM
Funding acquisition: JBM
Project administration: JBM
Supervision: JBM
Writing – original draft: DLB, JBM
Writing – review & editing: DLB, VEI, SJD, JBM

Competing interests: Authors declare that they have no competing interests.

Keywords

Vaccine; Adjuvant; Inflammasome; dmLT; MPL-A; T cells; Dendritic cells

Introduction

Infectious diseases are the leading cause of death in infants and children and the second leading cause of death worldwide (1–3). Vaccines are the most efficient tool in protecting people from infectious diseases, ideally conferring pathogen-specific sterilizing immunity that is long-lasting (4). Most vaccines consist of inactivated pathogens or recombinant subunits derived from non-living pathogen antigens, many of which are poorly immunogenic (5). To increase the immunogenicity of these antigens, adjuvants are added to vaccines where they can elicit potent immune responses, yet the majority of adjuvanted vaccines continue to utilize aluminum salts (alum), the adjuvant of choice for over 100 years. While alum excels at eliciting a potent antibody response, it is poor at inducing cell mediated immunity and thus is ineffective against a variety of intracellular pathogens, especially at the mucosal surface where a tissue specific Th1 and or Th17 T cell response would often be more desirable (6–8). Because only a few vaccine adjuvants are used in approved vaccine formulations in humans, there exists a limited repertoire of tools to tailor the most effective immune response during vaccination (9). We can address the need for novel adjuvants by combining two or more, well-characterized adjuvants with a vaccine antigen to generate a tunable, highly effective immune response that is best suited to control a particular pathogen. For instance, certain combinations could potentially allow us to exploit the properties of each individual adjuvant to elicit broad T and B cell immunity that can target cellular and humoral immunity to the mucosa, where most pathogens gain entry. Such an immune response would be particularly useful for the control of respiratory pathogens such as SARS-CoV-2 and influenza or intestinal pathogens such as Salmonella.

A variety of newer adjuvants have recently been assessed for use in the next generation of vaccines. For example, monophosphoryl lipid A (MPL-A), the biologically active lipid A portion of the gram-negative bacterial cell wall component lipopolysaccharide (LPS) or endotoxin, has garnered recent attention. While the immunomodulatory effects of LPS and MPL-A are similar, the latter exhibits approximately a 100-fold reduction in cellular toxicity making MPL-A an attractive vaccine adjuvant capable of inducing a robust immune response to co-administered vaccine antigens. MPL-A has been used in combination with alum for over a decade as the adjuvant AS04, which is used in the approved vaccine formulations for human papillomavirus (HPV) and hepatitis B (HBV) (10, 11). It is also used in combination with QS-21 in the shingles vaccine, Shingrix (12). Unlike LPS, which acts on toll-like receptor 4 (TLR4) and predominantly signals in a MyD88 dependent fashion, MPL-A signaling is primarily MyD88 independent and utilizes the TIR domain-containing adaptor inducing IFN-β (TRIF) to induce the production of type-I interferons and upregulate IFN-inducible genes (13). It is speculated that the reduced toxicity of MPL-A can be attributed to its MyD88 independence, which results in a less severe inflammatory response downstream of TLR4 signaling (14). Subsequently, TLR4 ligation activates nuclear factor kappa B (NF-κB) and protein kinase cascades that result in the

production of pro-inflammatory cytokines such as IL-12, TNF, IL-6, and pro-IL-1β and the subsequent polarization of, predominantly, Th1 CD4 T cells (12–14). While Th1 cells are efficient at combatting some infections, namely viral infections, other infections are resistant to Th1 immunity and so adjuvant choice can greatly affect vaccine efficacy. For example, we and others have shown that the ADP-ribosylating adjuvant double mutant heat labile toxin (dmLT) can promote both systemic and mucosal Th17 immune responses that are more effective at combatting infections caused by extracellular bacteria and fungi (15–18). Parenteral (intramuscular, intradermal, transcutaneous) delivery of dmLT avoids the reactogenicity which plagues the holotoxins, such as heat labile toxin and cholera toxin (17). dmLT is a classical AB_5 toxin with an enzymatic A-subunit that is non-covalently associated with a pentameric B-subunit. While the B-subunit is responsible for cellular entry via GM1 ganglioside binding, the A-subunit ADP-ribosylates Gsα, leading to the irreversible activation of adenylate cyclase, accumulation of intracellular cyclic adenosine mono phosphate (cAMP) and the activation of protein kinase A (PKA), all of which has been shown to be required for adjuvanticity (17–19). In addition to the cAMP-PKA axis, ADP-ribosylating adjuvant activity has been shown to potentially require caspase-1 (Cas1), inflammasome-dependent IL-1 signaling (16, 18).

The mechanism of action for many of these newer adjuvants remains unclear, particularly when combined. Some adjuvant combinations such as AS04, activate the inflammasome which are multiprotein complexes that assemble in the cytosol of epithelial and immune cells and involve the detection of Danger-Associated Molecular Patterns (DAMPs) or Pathogen Associated Molecular Patterns (PAMPs) (20–22). While there are several types of inflammasome complexes that sense distinct perturbations, their triggering results in the activation of caspases, particularly caspase-1, which subsequently cleaves and releases the active from of the inflammatory cytokines IL-1β and IL-18. Activated caspase-1 also cleaves and activates gasdermin D (GSDMD), a pore-forming protein that permeabilizes the plasma membrane, causing pyroptosis and allowing for the release of activated IL-1β as well as additional DAMPS (23–25). Because this event is highly inflammatory and can be detrimental to the host, this process is highly regulated and the initiation requires two steps, the first of which is priming (signal 1). In the context of the canonical inflammasome in innate immune cells, priming occurs during the sensing of microbial components, such as LPS, leading to the activation of NFkB and the subsequent upregulation of nod-like receptor family pyrin domain containing 3 (NLRP3) and pro-IL-1β (20). Once primed, the inflammasome is triggered by signal 2 which includes an array of stimuli including particulate matter such as salt crystals, extracellular ATP, pore-forming toxins, ionic flux, and mitochondrial or lysosomal damage. Once triggered, the inflammasome sensors NLRP3 and ASC (apoptosis-associated spec-like protein) interact and nucleate monomers of pro-caspase-1 which, when in close proximity to one another, initiates self-cleavage into active caspase-1 which can then cleave pro-IL-1β into biologically active IL-1β (20, 26). It is by this mechanism that the vaccine adjuvant AS04 likely works, where MPL-A acts as the priming event through TLR4 binding and alum is the trigger to initiate inflammasome assembly, resulting in a more potent and effective cellular and humoral immune response than if either adjuvant were used alone.

Despite the ability of MPL-A and dmLT to serve alone as potent vaccine adjuvants, there are no studies exploring the effect of the two as a combination adjuvant on antigen presenting cells such as dendritic cells (DCs) or on the resulting antigen-specific CD4 T cell response. In the present study, we investigated the potency of this adjuvant combination and assessed the mechanisms that might regulate the adjuvant effect of combining these adjuvants. We show that the combination of dmLT and MPL-A induces more robust activation of DCs compared to either adjuvant alone, leading to the activation of the NLRP3 inflammasome complex and increased secretion of IL-1β, as well as other hallmark pro-inflammatory Th1/2/17 polarizing cytokines. Unexpectedly, this inflammasome activation occurred independent of classical gasdermin D mediated pyroptosis. Furthermore, this adjuvant combination is most potent at expanding and activating multi-faceted Th1, Th2 and Th17 antigen specific CD4 T cells. These findings suggest this combination adjuvant can successfully be used as a novel platform to elicit protective immunity against a co delivered vaccine antigen(s) and this immunity is at least partially dependent on non-pyroptotic NLRP3 inflammasome activation.

Materials and Methods

Ethics Statement

This study was carried out in accordance with recommendations from the Guide for the Care and Use of Laboratory Animals of the National Institutes of Health. Tulane University is accredited by the Association for Assessment and Accreditation of Laboratory Animal Care (AAALAC). All experimental procedures involving animals were approved and performed in compliance with the guidelines established by Tulane University School of Medicine's Institutional Animal Care and Use Committee.

Animals

C57BL/6J, NLRP3 KO (B6.129S6-Nlrp3tm1Bhk/J), and Caspase-1 KO (B6.Cg-Casp1em1Vnce/J) mice were purchased from Jackson Laboratory (Bar Harbor, ME), and were maintained under specific-pathogen-free conditions in the vivarium at Tulane University School of Medicine. Mouse femurs from ASC KO and GSDMD KO mice were kindly provided by Dr. Igor Brodsky at the University of Pennsylvania, where they were shipped overnight at −20C in cRPMI-10% and processed immediately upon arrival at Tulane University.

Adjuvants and Reagents

dmLT (R192G/L211A) was produced from an *E. coli* clone expressing recombinant protein as previously described (27). Briefly, *E. coli* cultures were lysed in a microfluidizer, dialyzed and fractionated by D-galactose affinity chromatography. After elution, purified protein was passed through high-capacity endotoxin removal resin (Thermo) and stored lyophilized at 4C and freshly resuspended in ultrapure H_2O at a concentration of 1mg/ml prior to use. The endotoxin content of dmLT was measured using the chromogenic endotoxin quant kit (Pierce) and was determined to be 0.02 pg/μg protein. Commercially available MPL-A (Invivogen) extracted from LPS produced by *Salmonella Minnesota* was stored lyophilized at −20C, resuspended in DMSO at a concentration of 1 mg/ml, sonicated for 5 minutes and

vortexed for 1 minute immediately prior to use. LPS extracted from *Salmonella Minnesota* (Invivogen) was stored lyophilized at −20C, resuspended in ultrapure H_2O at a concentration of 2.5 mg/ml, sonicated for 5 minutes and vortexed for 1 minute immediately prior to use. ATP (Sigma) was resuspended in ultrapure H_2O at a concentration of 100 mM stored at −20C until ready to use. 2W1S peptide (sequence: EAWGALANWAVDSA) was purchased as sterile and endotoxin free from GenScript Biotech and resuspended at 4 mg/ml in sterile DPBS (Gibco) immediately prior to use.

Generation, Treatment and Preparation of Bone Marrow Derived Dendritic Cells

DCs were cultured and expanded from the bone marrow of mouse femurs, where the bone marrow was flushed, homogenized, and cultured for 7 days in the presence of 20 ng/ml rGM-CSF (Peprotech) in cRPMI-10% at 37C, 5% CO_2. For cytokine assays, suspension cells were harvested, washed, and plated in 96-well plates at 1.5×10^5 cells per well prior to treatment. For all other assays, cells were plated in 12-well plates at 1×10^6 cells per well prior to treatment. Cells were treated with escalating doses (0.01–100 μg) of dmLT, MPL-A, or a combination over the course of 1–48 hours. Positive controls consisted of treatment with 50 ng LPS for 24 hours for activation or for 3 hours with LPS plus an additional 45 minutes with 5 mM ATP for canonical NLRP3 inflammasome activation. For LDH controls, 10x lysis buffer for maximum LDH activity or dH_2O for spontaneous LDH activity was added 45 minutes prior to treatment endpoint. After treatments, DCs were centrifuged at 1,600 RPM at 4C and supernatant for ELISA, IFN-beta, cAMP, PGE_2 and LDH assays was collected and stored at −20C until ready to assay. For flow cytometry, DCs were washed with chilled PBS and single cell suspensions were subsequently processed for FACS analysis. For western blots, cells were washed 2x with chilled PBS and lysed for 5 minutes using CelLytic M (Sigma) supplemented with 1x protease/phosphatase inhibitor cocktail (Cell Signaling) and lysates stored at −20C until ready to assay. For RNA based experiments, cells were washed 2x with chilled PBS and further processed with RNEasy Plus Mini Kit (Qiagen) and RNA eluted in 50 μl ultra-pure water. RNA purity and concentration were determined on a Nanodrop 2000 (Fisher) and stored at −80C until ready to assay.

Cytokine ELISAs

Cell supernatants were assayed for IL-1β, IL-6, IL-12, and TNF secreted cytokines using 96-well flat bottom plates (Greiner Bio-one) each coated with the respective mouse anti-cytokine (Invitrogen: IL-1β: clone B122, IL-6: clone MP5–20F3, IL-12: clone C15.6, TNF: clone F3F3D4) and incubated for 1 hour at 25C. Next, wells were blocked with 2% BSA for 1 hour at 25C and then cytokine standards or 1:10 diluted supernatants in 2% BSA were added and incubated overnight at 4C. The next day, the respective mouse biotin anti-cytokine secondary antibody (Invitrogen: IL-6: clone MP5–32C11, IL-12: clone C17.8, TNF clone MP6-XT3, MP6-CT22, polyclonal IL-1β) was added for 1hr at 25C followed by the addition of 1:2000 Avidin-HRP in 2% BSA for 30 minutes at 25C. ELISAs were developed using KPL TMB Substrate system (Sera Care) and the absorbance read at 450 nm. Data was analyzed using a sigmoidal dose-response with least squares fit.

Cytotoxicity by lactate dehydrogenase activity

Cell supernatants were assayed for LDH cytotoxicity (Pierce) following manufacturer's instructions. Briefly, 50 μl of supernatant was added in triplicate to a 96-well flat bottom plate (Greiner Bio-one), followed by 50 μl of reaction mixture. The plate was incubated at 25C in the dark for 30 minutes before stopping the reaction with 50 μl of stop solution. The absorbance was read at 490 nm and 680 nm and % cytotoxicity was calculated per the equation:

$$\%\ Cytotoxicity = \frac{Adjuvant\ treated\ LDH\ activity - Spontaneous\ LDH\ activity}{Maximum\ LDH\ activity - Spontaneous\ LDH\ activity}\ x\ 100$$

Flow Cytometry

Single cell suspensions of BMDCs were prepared in flow sorter buffer (1x phosphate buffered saline, 2% newborn calf serum, and 0.1% NaN_3) and incubated in FcBlock with 2% mouse and rat serum for 10 minutes on ice before surface staining with antibodies at 1:100 dilutions for 30 minutes at 4C. Antibodies used for flow cytometry were as follows: eFluor450-CD11c, BV605-CD80, BV510-CD86, FITC-MHC-II, APC-CD40, PE-Cy7-CD11b, APC-ef780-Viability. DCs were classified as live cells that were highly positive for the lineage marker CD11c. To identify the population of 2W1S-specific CD4 + T cells, enriched cell suspensions were stained with viability APC-ef780, lineage negative (eFluor450- CD11b, CD11c, F4/80, and CD19), PE-Cy7-CD25, PerCP-Cy5.5-CD3, FITC-CD8α, and PE-CD44 antibodies. Cells were collected on a LSR Fortessa (Beckton-Dickson). Data were analyzed using FlowJo software (TreeStar). Tetramer-positive cells were gated as lineage negative (CD11b-, CD11c-, F4/80-, CD19-), CD3ε +, CD4 +, CD8α-, $CD44^{hi}$, and $I\text{-}A^b$:2W1S-APC +. Antigen specific cells were enumerated using Accucheck counting beads (Invitrogen) at a known concentration. The number of antigen-specific T cells was calculated by multiplying the total cell number with the percentage of tetramer-positive cells. All FACS data was analyzed using FlowJo™ v10.7.1 Software (BD Life Sciences).

Western Blot

Cell lysates were quantified for total protein concentration using Coomassie Plus assay kit (Pierce) and 15 μg of protein was loaded into each well of a 4–12% Bis-Tris 12-well gel (NuPage). Gels were run at 200V for 45 minutes and then transferred to a nitrocellulose membrane using iBlot transfer stacks (Thermo). Successful transfer was verified by ponceau stain and then membranes were blocked with 5% BSA in PBS-T for 1 hour at 25C. Secondary antibodies from Cell Signaling were added at 1:1000 in 5% BSA in PBS-T and incubated overnight at 4C and are as follows: rabbit anti-mouse- IL-1β (31202), cleaved-IL-1β (63124), caspase-1 (24232), cleaved caspase-1 (89332), NLRP3 (15101). Rabbit anti-mouse β-actin (BioLegend 622102) was added at 1:1000 as a normalization control. Anti-rabbit IgG-HRP detection antibody (7074) was added at 1:2000 in 5% BSA in PBS-T and incubated for 1 hour at 25C. Blots were developed using SignalFire ECL reagent (Cell Signaling), imaged on an Amersham 600 Imager (GE), and bands quantified using ImageJ v1.8.0.

RNA Sequencing and identification of signal transduction pathways

Total RNA was used for deep sequencing using the Illumina TruSeq RNA sample guide (v2). Briefly, mRNA was purified with oligo(dT) beads, fragmented with magnesium and heat-catalyzed hydrolysis, and used as a template for first- and second-strand cDNA synthesis with random primers. The cDNA 3′ ends were adenylated, followed by adaptor ligation and a 15-cycle PCR to enrich DNA fragments. Quantification of cDNA libraries was performed by using a Kapa Biosystems primer premix kit with Illumina-compatible DNA primers. The cDNA libraries were pooled at a final concentration 1.8 pM. Single-read sequencing was performed on an Illumina Genome Analyzer IIx and NextSeq 500. Sequencing reads were annotated and aligned to the UCSC mouse reference genome (GRCm38/mm10) using RNA-seq Aligner STAR (28). Functional analysis was performed on differentially expressed genes in each time point and were uploaded and analyzed separately using the software package IPA (Ingenuity Systems, Redwood City, CA, USA). The resulting biological functions, canonical pathways, and upstream regulators were filtered by setting a threshold of $P < 0.05$ using Fisher's exact test.

RT-qPCR

Total RNA was used to generate cDNA by adding 100 ng of pure RNA to the iScript cDNA synthesis kit (Bio-Rad) and all primers were purchased from IDT. Blank and no reverse transcriptase controls were included to ensure primer specificity. A reaction mixture containing 200 μM each primer and 1 μl of cDNA was added to the iQ SYBR green Supermix (Bio-Rad) and RT-qPCR was performed using the CFX Connect real-time PCR machine (Bio-Rad). Data was analyzed using the $\Delta\Delta C_T$ method, normalizing all samples to GAPDH and comparing relative expression levels to those of untreated cells.

Type-1 interferon multiplex

BMDC supernatants were assessed for the secretion of the interferon β after treatment with single and combination adjuvant using the IFN alpha/beta mouse ProcartaPlex panel. Briefly, treated BMDC supernatant was collected at 1, 2, and 6 hours post treatment and 50ul supernatant was applied per well following manufacturers recommendations. Data was collected using the Bio-Rad Bioplex-200 system and analyzed using a 5-parameter curve fit.

cAMP Accumulation and Detection

BMDCs were cultured from the bone marrow of C57BL/6 mice and differentiated using recombinant GM-CSF. Cells were seeded in 6 well plates at a concentration of 1×10^6 cells/mL in cRPMI-10% and stimulated with 10μg/mL dmLT, MPL, or in combination for 24 hours at 37C, 5% CO_2. After 21 hours, the phosphodiesterase (PDE) inhibitors rolipram and cilostazol were added at 50μM to prevent conversion of the secondary messenger cAMP. Heat-labile toxin from *E. coli* (LT) was included as a positive control, while unstimulated cells were only treated with PDE inhibitors. Total responses were determined by analyzing both the supernatants and cell lysates using the cAMP Parameter Assay Kit (R & D Systems) as per manufacturers recommendation.

Detection of PGE_2

BMDC cell supernatants were assessed for the secretion of the PGE_2 after treatment with single and combination adjuvant for 24 hours using the Prostaglandin E2 Parameter Assay Kit (R & D) Systems) as per manufacturers recommendation.

Immunizations, Tissue Processing and Enrichment of Antigen-specific CD4 T cells

C57BL/6 mice were immunized intradermally in the ear with a single dose of 10μg of the model antigen 2W1S +/− 1μg dmLT, 1μg MPL-A, or a combination of the two. 10 days later the CLNs were harvested, and single cell suspensions were obtained by homogenization through a 100 mm nylon mesh filter in cold sorter buffer (1 × phosphate buffered saline, 2% newborn calf serum, 1 mM EDTA, and 0.1% sodium azide) and resuspended in FC block (Clone 2.4G2 SFM supernatant + 2% mouse serum, 2% rat serum, 0.1% NaN3) prior to incubation with 10 nM $I\text{-}A^b$:2W1S-APC MHC-II tetramer in the dark for one hour at room temperature. 2W1S-specific T cells were enriched by magnetic separation with anti-APC magnetic beads (Miltenyi) as described previously. Briefly, cell suspension was incubated with anti-APC microbeads for 30 min on ice in the dark. Cells were then washed, resuspended in cold sorter buffer, and applied to Miltenyi LS Columns placed on a quadroMACS magnet over a nylon mesh. The columns were rinsed two more times with cold sorter buffer. 2W1S tetramer-bound cells were released from the columns by addition of cold sorter buffer to the columns off the magnet and subsequently processed for analysis by flow cytometry.

Statistical Analysis

Primary statistical analyses were performed using Graphpad Prism v9 by ordinary one-way analysis of variance (ANOVA) with Tukey's multiple comparison test or two-way ANOVA with Dunnetts or Sidak's multiple comparison test to determine statistical significance and p values, as appropriate. Significant differences were noted as *, $p<0.05$; **, $p<0.01$; ***, $p<0.001$; ****, $p<0.0001$ and are displayed on figures. For selected cell count and secreted cytokine results, secondary analyses were performed to test for an interaction between dmLT and MPL-A treatments. Linear regressions including terms indicating if an animal had been treated with dmLT or MPL-A, alone or in combination, and an interaction between treatments were performed using R v4.2.0 and are shown in Table 1.

Results

The adjuvant combination of dmLT and MPL-A increases the expansion and activation of Th1, Th2, and Th17 antigen-specific CD4 T cells.

To determine if the combination of dmLT and MPL-A (hereafter combination adjuvant) would be a viable candidate for use in a vaccine formulation, we immunized wild type (WT) C57BL/6 mice intradermally with the model CD4 T cell antigen 2W1S with and without dmLT, MPL-A or a combination of the two. Ten days later we used an $I\text{-}A^b$:2W1S MHC-II tetramer to assess endogenous 2W1S-specific CD4 T cell expansion and activation as well as the functional phenotype of these cells as previously described (Fig S1) (29). To ensure the 2W1S-specific CD4 T cells were specifically recognized by the tetramer,

we initially immunized mice with the adjuvant combination alone in the absence of 2W1S antigen and enriched for tetramer binding cells in the injection site draining cervical lymph nodes (CLNs). As shown in Fig S1B, we found that only naïve ($CD44^{lo}$) 2W1S-specific T cells were detected by the tetramer at very low numbers (average 127± 17.25 naïve cells from 5 mice) as has been reported by ourselves and others (30–32). This gave us confidence that the tetramer was truly detecting all the 2W1S-specific CD4 T cells in subsequent immunization experiments. Interestingly, we found that MPL-A did not appreciably increase antigen-specific T cell expansion in the draining CLNs when compared to 2W1S alone; however, immunization with dmLT resulted in an increase in expansion in the CLNs, which resulted in a multiplicative effect ($p = 0.002$) by the addition of MPL-A that was not explained by adding the two results together (Fig 1 A−B). The results of this effect are shown in Table 1 where the significant interactions between MPL-A and dmLT are delineated. To determine whether these antigen specific CD4 T cells were activated, we assessed cells for the expression the early activation marker CD25. Again, we found that immunization with the combination adjuvant resulted in the greatest number of CD25 expressing antigen-specific CD4 T cells (Fig 1 C−D). We have previously shown that dmLT can induce mucosal gut CD4 T cell immunity following parenteral (intradermal) administration that induces upregulation of the gut homing integrin α4β7 on CD4 T cells in the draining lymph nodes (15), so we next investigated how the combination adjuvant effected the expansion of these cells. Surprisingly, antigen-specific α4β7+ CD4 T cell expansion was exclusively dmLT mediated where the addition of MPL-A had no impact on this response (Fig S1 C−D). This data suggested that the combination adjuvant is most efficient at expanding and activating vaccine specific CD4 T cells in the draining CLNs and that the inclusion of dmLT in our vaccine formulation continues to allow for the engagement and expansion of mucosal gut homing phenotype $\alpha 4\beta 7 +$ CD4 T cells. Vaccine responses are often assessed in terms of the humoral immune response. While not the focus of this study, we nonetheless assessed whether a single priming immunization with each adjuvant or the combination had any effect on antigen-specific antibody responses 10 days after immunization by analyzing 2W1S-specific serum IgG. As expected, because the 2W1S antigen we used is a peptide, no 2W1S-specific antibodies were observed in serum (Fig. S2E). We did find dmLT-specific IgG in the serum of vaccinated mice where once again; the combination displayed the greatest amount of antibody. It has been reported that these anti-dmLT antibodies do not affect subsequent adjuvanticity (33). dmLT is an attractive adjuvant because it elicits a multi-faceted Th1/2/17 CD4 T cell immune response following immunization. MPL-A has been described to induce predominantly Th1 responses, so we next sought to determine how the combination adjuvant would affect T cell polarization. To do this, we assessed cytokine secretion from tetramer enriched 2W1S-specific CD4 T cells from the CLN stimulated with 2W1S antigen for 72 hours. We found that 2W1S-specific CD4 T cells from CLNs of mice immunized with 2W1S with or without MPL-A did not exhibit an appreciable recall response to 2W1S (Fig 2); however, animals immunized with dmLT and the combination adjuvant displayed a mixed Th response and secreted cytokines associated with Th1 (IL-2, IFNγ), Th2 (IL-5, IL-13), and Th17 (IL-17A, IL-22) polarization, with the combination adjuvant exhibiting the highest level of secretion for the majority of cytokines assessed. Additional testing of the interaction between dmLT and MPL-A indicated a significant interaction between dmLT and MPL-A for these cytokines

that was not simply explained as an additive effect. The statistical results of this interaction are shown in Table 1. Together this data demonstrated that the combination adjuvant is capable of successfully eliciting the most potent multi-faceted antigen specific CD4 T cell response in the draining cervical lymph nodes in response to intradermal vaccination.

Combination adjuvant differentially alters the transcription profile and activates the inflammasome pathway in DCs.

Because DCs are abundant at sites of immunization and largely responsible for the initiation of the CD4 T cell response, we sought to determine how dmLT, MPL-A, or the combination adjuvant effects gene expression in DCs to gain insight into how these adjuvants might modulate the subsequent adaptive immune response (34). To do this, bone marrow derived DCs (BMDCs) were treated for 24 hours in vitro with each individual adjuvant or the combination and then adjuvant-induced changes to the transcriptome was determined using RNA-seq. The number of genes differentially regulated in BMDCs treated with dmLT was 753; with MPL-A it was 279, and in the combination, it was 896 genes (Fig 3A). Using Qiagen ingenuity pathway analyses we identified relationships between gene signatures and predicted the activation state of various pathways in the DCs. The MIF regulation of innate immunity, Th1/2/17, interferon (IFN), toll-like receptor (TLR), protein kinase A (PKA), inflammasome and NF-κB were among the top activated pathways (Fig 3B). Among the genes that were significantly upregulated in the combination adjuvant treatment were those associated with cell survival and T cell immunity (PRDX1, TNFSF11, TNFRSF1B, CD80, CD86, CD40), TLR signaling (TLR4, CD14, TRAFD1, TRAF6, IRF1), inflammasome signaling (IL1R1, IL1A, IL1B, Casp1, NLRP3), T helper cell polarization (IL12A, IL6, Tgfb1/2), and cAMP and prostaglandin signaling (PRKAR2A, PDE4C, PTGES, PTGS2, PTGER2) (Fig 3C). Using the IPA upstream regulator analysis, we identified IL-1β as a key transcriptional regulator within our gene expression dataset (Fig 3D). This data suggested that the combination of dmLT and MPL-A acts through TLR4 and PKA in DCs to initiate a multifunctional, hyperactivated response that is potentially mediated by the canonical NLRP3 inflammasome followed by the subsequent release of IL-1β.

Caspase 1, NLRP3, IL1b, and GSDMD mRNA expression in DCs is temporally regulated after treatment with combination adjuvant.

Identifying that the inflammasome pathway was activated in DCs after a 24-hour treatment with the combination adjuvant and finding that IL-1β was predicted to be a major contributor to transcriptional regulation, we next sought to understand the temporal expression of inflammasome genes in DCs. Cells were treated for 1, 2, 3, 6, 12, and 24 hours with single or combination adjuvants and then caspase-1, NLRP3, IL-1β, and gasdermin D gene expression was measured using RT-qPCR and fold-change was normalized to GAPDH. We found that NLRP3 and caspase-1 peak expression occurred 6 hours post stimulation with the combination adjuvant, that IL-1β expression peaked by 12 hours, but that expression of gasdermin D was minimal over the entire time course (Fig 3D), suggesting that the secretion of IL-1β may be independent of classical inflammasome pyroptosis. Furthermore, using the secreted alkaline phosphatase reporter system (SEAP), we found that both dmLT and MPL-A independently caused activation and translocation of NF-κB over the span of 72 hours and that the combination does this to a significantly greater extent (Fig S2A). Together

this data demonstrated that DCs undergo a priming event to initiate the expression of NF-κB and the canonical inflammasome genes NLRP3, caspase-1, and IL-1β upon stimulation with the combination adjuvant and exhibited the greatest potential for inflammasome activity and release of active IL-1β compared to either adjuvant alone.

The combination adjuvant increases the production of intracellular NLRP3, both pro- and active Caspase 1, IL-1β, cAMP, PGE_2, and COX II.

To verify that observed gene expression was reflected in protein synthesis, we next sought to determine whether the combination adjuvant could drive the production of the NLRP3 protein and both the inactive pro and active cleaved forms of caspase-1 and IL-1β by western blot (Fig 4A). We found that NLRP3 was upregulated after a 24-hour stimulation with each adjuvant but was highest in BMDCs treated with MPL-A, either alone or in combination with dmLT (Fig 4B). We also found the greatest level of both pro- and active caspase-1 in BMDCs treated with the combination adjuvant (Fig 4C−D), suggesting that the NLRP3 inflammasome complex is assembled and has converted pro-caspase-1 to functionally active caspase-1 after exposure to the combination adjuvant. Intracellular pro-IL-1β (Fig 4E) was produced at low levels in cells treated with dmLT or MPL-A alone, with the greatest response occurring upon treatment with the combination adjuvant; however, fully functional cleaved IL-1β (Fig 4F) was absent in cells treated with dmLT and was very modest after MPL-A treatment. In contrast, active IL-1β was greatest after treatment with the combination adjuvant suggesting that DCs treated with the combination adjuvant produce the inflammasome proteins NLRP3, pro-caspase-1 and pro-IL-1β upon stimulation and within 24 hours assemble the NLRP3 inflammasome to convert pro-caspase-1 to active caspase-1, which subsequently converts pro-IL-1β to active IL-1β. Based on these results, these cells were either able to continue the production of both pro- and active IL-1β and/or sequester it in the cytosol over a 24-hour period, which runs counter to canonical inflammasome pyroptosis and release of cleaved IL-1β. Since it is known that cAMP has an inhibitory effect on the NLRP3 inflammasome and because dmLT relies on the induction of low levels of cAMP for adjuvanticity, we next sought to determine how the addition of MPL-A would affect cAMP production. BMDCs were treated as before with each adjuvant individually or in combination and cAMP was assessed. We found that the combination adjuvant induced the highest amount of cAMP at 24 hours compared to either adjuvant alone (Fig 4G). Since addition of MPL-A to dmLT increased intracellular cAMP production, we hypothesized that the eicosanoid prostaglandin E_2 (PGE_2) and the enzyme cyclooxygenase-2 (COX-2), known to be upregulated by TLR4 ligation, contribute to downstream cAMP-PKA signaling. As expected, both intracellular COX-II (Fig 4H) and secreted PGE_2 levels (Fig 4I) were highest in cells stimulated for 24 hours with the combination adjuvant and for PGE_2 this level showed a significant interaction between the two adjuvants that could not be explained by adding the results from each alone (Table 1). Because inducible type-1 interferon genes were upregulated in our RNA sequencing analysis, we next sought to determine how the adjuvants affected secretion of IFNβ, another cytokine shown to negatively regulate inflammasome activity. We found that MPL-A significantly increased secretion both alone and in combination with dmLT over the course of 6 hours (Fig S2B). These findings contradict published observations that IFNβ, cAMP, and more specifically

PKA signaling, negatively regulates the NLRP3 inflammasome and downstream processing of pro-IL-1β to the active form.

Activation of DCs is NLRP3 dependent, but Caspase 1 and GSDMD independent.

To understand how single and combination adjuvants affect the phenotype of DCs and whether the NLRP3 inflammasome is required for full activation of these cells, we treated BMDCs derived from wild type (WT) C57BL/6, NLRP3 Knockout (KO), ASC KO, Cas1 KO, and gasdermin D KO mice with each adjuvant alone or in combination for 24 hours and subsequently analyzed a variety of activation-induced surface markers (Fig 5A). We found that the combination adjuvant imparted the greatest surface expression of CD40, CD86, and MHC-II in WT cells (Fig 5B) and that these elevated levels were maintained in caspase-1 KO (Fig 5C cells but were slightly attenuated in ASC KO cells (Fig 5D). In contrast, there was no significant increase in CD40 or CD86 and only a slight increase in MHC-II expression in NLRP3 KO cells (Fig 5E), demonstrating that NLRP3 is likely required for DCs to either become activated or maintain an activation phenotype for 24 hours post stimulation. Notably, even the single adjuvant treatments effects were attenuated in NLRP3 KO cells indicating that this outcome was broad. As the canonical inflammasome generally results in gasdermin D mediated pyroptosis and the subsequent release of intracellular cleaved IL-1β, we expected BMDCs derived from GSDMD KO animals to display an activation defect. Surprisingly, we found that GSDMD is ultimately dispensable for combination adjuvant induction of DC activation (Fig 5F) showing that the combination adjuvant is most effective at activating DCs and that this activation is NLRP3 dependent but is Caspase-1 and GSDMD independent.

IL-1β secretion requires key components of the NLRP3 inflammasome complex but is GSDMD independent.

Since RNA expression indicated that pathways associated with Th1, 2 and 17 polarizing cytokines were activated, we next sought to determine if DCs derived from inflammasome KO animals would have a defect in their ability to produce and secrete the hallmark Th polarizing cytokines IL-1β, IL-6, IL-12, and TNF after stimulation with single or combined adjuvants. We found that WT DCs secreted IL-6, IL-12, and TNF in response to MPL-A regardless of whether it was combined with dmLT. This trend held true in DCs derived from NLRP3 KO, ASC KO, Cas1 KO, and GSDMD KO animals (Fig 6A). As expected, IL-1β secretion in WT DCs (Fig 6B) displayed a multiplicative effect after treatment with the combination adjuvant (Table 1). Moreover, IL-1β was completely ablated in NLRP3 KO, ASC KO, and Cas1 KO DCs (Fig 6C); however, this was not true for DCs derived from GSDMD KO animals, where IL-1β secretion was unaffected by the absence of gasdermin D. Because classical inflammasome activation typically results in pyroptosis, we next sought to determine if the increase in IL-1β secretion after treatment with the combination adjuvant was due to increased cell death. We found that neither dmLT, MPL-A, or the combination induced significant cell death in DCs after treatment for up to 24 hours when compared to untreated controls (Fig 6D). This data indicates that the loss of the NLRP3 inflammasome complex does not affect the ability of the combination adjuvant to induce production of typical proinflammatory cytokines like IL-6, IL-12 and TNF, but that it is essential for IL-1β secretion. Additionally, GSDMD is not required for the secretion of

IL-1β, indicating that the inflammasome is operating independently of classical pyroptosis and subsequent cell death. Because we observed increased inflammasome activity in our combination adjuvant treated BMDCs, we sought to determine the role of dmLT in the 2-step process of inflammasome signaling. It is well established that LPS and its derivative MPL-A prime the canonical inflammasome and we found that DCs primed with dmLT and subsequently treated with ATP secrete IL-1β, indicating that dmLT may in fact also be contributing to the priming (signal 1) step (Fig S3A). To ensure that our observations weren't due to residual LPS contamination in our dmLT stock, we rigorously removed endotoxin such that the level was 0.02 pg/μg protein. Since it has been shown that CT and LT can modulate TLR signaling, we wanted to test if the secretion of IL-1β in our combination adjuvant treated BMDCs was dose dependent (16). Additionally, because LPS can activate the inflammasome independent of TLR signaling (35), we wanted to verify that the loss of TLR4, using TLR4 KO BMDCs, would ablate cytokine secretion. We found the optimal dose of dmLT to be 10ug/ml, where additional dosing of MPL-A impacted the magnitude of IL-1β secretion with the optimal dose being 1ug/ml (Fig S3B) and that TLR4 ligation is essential for our combination adjuvant to elicit cytokine responses (Fig S4). This suggests that the extent of IL-1β secretion is TLR4 dependent and can be controlled with the addition of MPL-A in a dose-dependent fashion.

Discussion

Infectious diseases remain one of the leading causes of death worldwide and with the increasing threat of newly emerging pathogens, there is a need for novel and improved vaccines, particularly those that can induce multipotent mucosal immunity. Adjuvants are essential for the development of many effective vaccines, yet only five adjuvants have been used in humans in approved vaccine formulations since the discovery of alum in the 1920's and they are limited in their ability to induce a protective cellular or mucosal immune response. For example, MF59, an oil-in-water emulsion containing squalene, has been successful in increasing antibody titers to coadministered influenza antigen in the Fluad vaccine (36). Both Alum and MF59 function by inducing the secretion of chemokines at the immunization site which results in the recruitment and activation of antigen presenting cells, increased migration to the draining lymph nodes and antigen presentation to the adaptive arm of immunity (6, 36, 37). While these adjuvants are effective at recruiting innate immune cells to the site of immunization via local chemokine secretion in the tissue, they alone do not have a substantial direct immunological effect on DCs and macrophages and often result in a non-biased Th response (MF59) or Th2 skewed polarization (Alum) (38, 39). Alternatively, the synthetic bacterial and viral DNA analogue CPG 1018, used in the hepatitis B vaccine Heplisav-B, is capable of polarizing Th1 responses and driving cellular immunity to co-administered vaccine antigens (40, 41). CPG 1018 has been shown to directly modulate DC and B cell functionality through TLR9 ligation, enhancing the activation and antigen presentation capacity of DCs which results in the generation of antigen specific Th1 CD4 T cells and CTLs, as well as the proliferation and polyclonal activation of B cells and the generation of plasma cells (40, 42). TLR engagement is a highly effective method of cellular activation since the downstream signaling processes are reflective of an active infection. Because the discovery of new adjuvants that are both safe

and effective has been difficult, some newer vaccines are exploring combining existing adjuvants to elicit potent responses. For example, the shingles vaccine Shingrix consists of zoster antigen adjuvanted with $AS01_B$, which is a combination of MPL-A and QS-21 (43). Because MPL-A mimics endotoxin found on the surface of gram-negative bacteria, it can initiate a cascade of pro-inflammatory events through ligation with TLR4 on a variety of cell types and predominantly polarizes Th1 immunity. Unlike MPL-A, adjuvanticity by the saponin QS-21 is not mediated through cellular receptors but is simultaneously endocytosed with antigen and promotes Th1 immunity although its use has been limited due to local reactogenicity (44, 45). Another combination adjuvant, AS04, consisting of co-adsorbed alum and MPL-A, is used in the HPV and HBV vaccines to improve both humoral and cell-mediated immunity. While alum is poor at eliciting a Th1 cellular immunity, the addition of MPL-A aids in inducing a mixed Th1 and Th2 response. $AS01_B$ and AS04 are prime examples of how combination adjuvants can exploit characteristics of each individual adjuvant, whether through TLR ligation or receptor independent mechanisms, to generate a more potent and tailored immune response.

Here we show that the combination of the adjuvants dmLT and MPL-A acts in a multiplicative manner causing a significant interaction between the two that can't be explained by simply adding the effects of the two adjuvants together to increase vaccine-specific CD4 T cell immunity and NLRP3 dependent, GSDMD independent activation and secretion of IL-1β in BMDCs. While not yet used in licensed human vaccines, dmLT is currently in the clinical trial pipeline and has not only been demonstrated to be safe and efficacious but, unlike many other adjuvants, can induce both systemic and mucosal antigen-specific humoral and cellular immune response even when administered parenterally. We have previously shown that this occurs when dmLT engages skin CD103+ dendritic cells inducing upregulation of the gut homing integrin α4β7 on CD4 T cells (15). The ability of AB_5 ADP-ribosylating proteins such as dmLT to activate DCs to polarize a Th17 cellular response has been shown to require both cAMP as well as IL-1 receptor signaling (17, 18). In our study, dmLT alone only slightly induces the expression of NLRP3, Caspase-1 and IL-1β and is unable to induce DCs to process and secrete/release active IL-1β. DCs primed with dmLT and subsequently treated with ATP secrete IL-1β, indicating that dmLT may in fact be contributing to the priming step (signal 1) in the inflammasome pathway. Previous studies show that other ADP ribosylating, enzymatically active AB_5 proteins such as CT and LT do not elicit cytokine secretion in murine BMDCs on their own but are capable of modulating responses to TLR agonists such as LPS (16, 46).

Furthermore, we observed that treatment of BMDCs with the combination adjuvant increased the production of cAMP, which may be attributed to the activation of the arachidonic acid pathway. We found that there was an increase in production of the cyclooxygenase COX-2, which is required for the conversion of arachidonic acid into the functional messenger prostaglandin E_2 (PGE_2). One of the ways PGE_2 can signal is through the prostaglandin surface receptors EP_2 and EP_4 and it has been shown that PGE_2 can both suppress the ability of DCs to make pro inflammatory cytokines but can also synergize with TNF to upregulate synthesis of IL-1β (47). Like dmLT, PGE_2 results in the in ribosylation of Gsα, the irreversible activation of adenylate cyclase, and the accumulation of intracellular cAMP (47–51). Interestingly, cAMP has been shown to be

necessary for dmLT to function as a vaccine adjuvant but has also been shown to negatively regulate inflammasome activity by both directly binding to NLRP3 to inhibit inflammasome assembly and through downstream PKA activity (52). Contrary to these findings, we observed that the increase in cAMP in our combination adjuvant treated BMDCs coincided in an increase in NLRP3 inflammasome related gene signatures, protein synthesis and secretion of the effector proinflammatory cytokine IL-1β. Additionally, the combination adjuvant increased both intracellular and secreted cAMP in BMDCs, the latter of which is likely converted to adenosine mono phosphate (AMP) in the extracellular milieu by CD39 and then ultimately metabolized to adenosine by CD73 (53, 54). Both CD39 and CD73 are ectophosphodiesterases that were found to be upregulated in our study via RNA sequencing. AMP has been shown to increase DNA synthesis, mitogenesis, F-actin polymerization, chemotaxis, and CD80/86 surface expression, while adenosine has been shown to have regulatory/immunosuppressive effects. It is possible that dmLT induces enough secreted cAMP that it can initiate the AMP pathway via CD39, but then is quickly converted to adenosine by CD73 upon which this activity is lost; however, since the combination of dmLT and MPL-A results in much higher levels of cAMP compared to dmLT alone, this potentially allows the pathway to remain active longer. We speculate that the AMP pathway may be contributing to the robust proinflammatory innate immune responses observed in BMDCs in our study, while the CD39/73 axis imparts a balanced Th1/2/17 polarizing phenotype on these cells (54).

Additionally, both MPL-A alone as well as the combination adjuvant stimulate BMDCs to secrete the type-1 interferon IFNβ, another factor that has been shown to negatively regulate NLRP3 inflammasome activity. Despite the increases in cAMP and IFNβ, the combination adjuvant increases NLRP3 inflammasome activity and the secretion of active IL-1β compared to unstimulated controls; however, the levels are substantially lower than BMDCs stimulated with the canonical inflammasome activators LPS and ATP, which relies on GSDMD mediated pyroptosis. It is possible that the combination adjuvant induces low level inflammasome activity that is more tightly regulated by cAMP and PKA signaling, type-1 interferons, and the self-limiting properties of caspase-1 (55), which leads to longer duration of cytokine secretion albeit with less cytotoxicity. We further observed that the combination adjuvant mediated activation of BMDCs was partially dependent on NLRP3, less so on ASC, and completely independent of caspase-1 and gasdermin-D. This is intriguing considering that we also showed that IL-1β secretion is completely ablated in BMDCs lacking NLRP3, caspase-1, or ASC, thus identifying a disconnect between cellular activation and IL-1β secretion. This is intriguing given that it has been shown that, in macrophages, caspase-1 dependent cleaved IL-1β relocates from the cytosol to the plasma membrane where it associates with the phospholipid phosphatidylinositol 4,5-bisphosphate (PIP2) and is subsequently released in the active form from the cell (56). This can occur in a gasdermin D independent manner and may partly explain what we observe here although that requires further investigation. Most surprising was the finding that expression of gasdermin D was minimal over the entire time course, suggesting that the secretion of IL-1β may be independent of classical inflammasome pyroptosis. The non-pyroptotic inflammasome has only recently been identified and attributed to a specialized subset of phagocytes termed “hyperactivated” (57, 58). These cells are

unique in that they have increased capacity for antigen uptake and presentation, are hyper-migratory via CCR7, are long-lived despite inflammasome activity and their phenotype is NLRP3, caspase-11, and gasdermin D dependent (59). In this case, gasdermin D activity is substantial enough for IL-1β release, but minimal enough for cells to repair the cell membrane and maintain viability (60). The implications of our finding are significant because the combination adjuvant is upregulating expression of genes associated with the NLRP3-Caspase-1 inflammasome, but secretion of IL-1β appears to be completely independent of gasdermin D (59). Interestingly, PGE_2 has been shown to be a key factor for CCR7 mediated migration of DCs from the skin to the lymph nodes and increases their T cell stimulatory potential and Th1 polarization (61). Our BMDC RNA sequencing data shows that the combination adjuvant increased CCR7 expression by nearly 3.5-fold, and upregulated genes and pathways associated with costimulation and migration capacity. This finding, along with the fact that treatment of BMDCs with the combination adjuvant increases both PGE_2 and cAMP and that immunization with the combination adjuvant results in significant expansion and activation of antigen specific CD4 T cells, shows that the combination adjuvant potentially imparts a hyperactivated phenotype on DCs at the immunization site. These hyperactivated DCs may then be primed to activate vaccine specific CD4 T cells via increased antigen presentation and costimulation. One potential advantage for the ability of the combination adjuvant to activate the inflammasome in DCs in the absence of pyroptosis is that this likely contributes to the robust antigen specific CD4 T cell responses seen after immunization as this allows for DCs to maintain the ability to present vaccine antigens to T cells without being eliminated as antigen presenting cells. This advantage extends to the ability for DCs to continue to produce T cell polarizing cytokines such as IL-1β that offers sustained activation of these T cells. This likely contributes to the overall increased expansion of vaccine specific T cells in our study over and above what would be predicted by simply adding tother the T cell numbers from either dmLT or MPL-A alone. Perhaps this is not surprising as neither of these adjuvants on their own has the capacity to activate the non-pyroptotic inflammasome and thus cannot sustain the requisite inflammatory cytokine production. As a vaccine, increasing T cell numbers is likely to offer increased and sustained protection against a variety of pathogens which is also advantageous. Indeed, this concept has already been proposed for increasing T cell responses to combat tumors and can also be applied here (62).

While we believe that this study adds to a growing body of knowledge regarding how the non-pyroptotic inflammasome can be activated, it is not without caveats. One weaknesses of the current study are the relatively small sample sizes in some experiments, although this is somewhat counterbalanced by repeated measures. Additionally, although mice serve as an excellent tool for assessing immune responses at a basic mechanistic level, it is not always clear how well such experiments might translate into human trials as it is known that preclinical vaccine models are not always predictive of human outcomes. A strength of our study is the demonstration of in vitro inflammasome involvement using multiple approaches including RNAseq to identify inflammasome related gene expression in the combination adjuvant treated DCs which were confirmed using several inflammasome pathway knockouts. Taken together we found that combining two potent, yet mechanistically different adjuvants together to induces a more potent and tailored innate immune response

that can then initiate multi-faceted CD4 T cell immunity. Because of the mucosal homing properties following parenteral immunization with dmLT and the increased expansion and activation of antigen-specific CD4 T cells with the addition of MPL-A, our combination adjuvant could be a great candidate for use in the next generation of respiratory vaccines such as those directed against SARS-CoV-2. Further, this combination has the potential to combat a variety of infections across multiple mucosal sites of entry. In addition to driving vaccine specific immunity to the mucosa, the combination adjuvant could also potentially allow for dose-sparing of vaccine antigen, which is often a limiting reagent in vaccine production. As we begin to understand how these adjuvants work together, we can use them as a tool to manipulate the immune response in the most effective manner against a wide array of existing and emerging pathogens.

Supplementary Material

Refer to Web version on PubMed Central for supplementary material.

Acknowledgments

We thank C. Flemington, Alanna G. Wanek, J.K. Kolls and the Tulane Center for Translational Research in Infection and Inflammation for their help with the RNA-seq studies. We thank Dr. L.A. Morici for thoughtful reading of the manuscript and Dr. I. Brodsky at the University of Pennsylvania for scientific guidance and for providing bone marrow from NLRP3, ASC, Cas1/11, and GSDMD KO animals for the inflammasome studies.

Funding

This study was funded by the National Institute of Health (NIH) grant U01AI124289 (JBM)

Data and materials availability:

All data are available in the main text or the supplementary materials. The RNA-seq data set generated in this publication has been deposited in the NCBI database under BioProject accession number PRJNA817578. https://www.ncbi.nlm.nih.gov/bioproject/PRJNA817578

References

1. Michaud CM 2009. Encyclopedia of Microbiology (Third Edition). Pathogenesis Article Titles G 444–454.
2. 2019. Standing up to infectious disease. Nat Microbiol 4: 1–1. [PubMed: 30546101]
3. Levine MM, Kotloff KL, Nataro JP, and Muhsen K. 2012. The Global Enteric Multicenter Study (GEMS): Impetus, Rationale, and Genesis. Clin Infect Dis 55: S215–S224. [PubMed: 23169934]
4. Doherty M, Buchy P, Standaert B, Giaquinto C, and Cohrs DP 2016. Vaccine impact: Benefits for human health. Vaccine 34: 6707–6714. [PubMed: 27773475]
5. Francis MJ 2018. Recent Advances in Vaccine Technologies. Vet Clin North Am Small Animal Pract 48: 231–241.
6. HogenEsch H. 2013. Mechanism of Immunopotentiation and Safety of Aluminum Adjuvants. Front Immunol 3: 406. [PubMed: 23335921]
7. Khader SA, and Gopal R. 2010. IL-17 in protective immunity to intracellular pathogens. Virulence 1: 423–427. [PubMed: 21178483]
8. Li Y, Wei C, Xu H, Jia J, Wei Z, Guo R, Jia Y, Wu Y, Li Y, Qi X, Li Z, and Gao X. 2018. The Immunoregulation of Th17 in Host against Intracellular Bacterial Infection. Mediat Inflamm 2018: 6587296.

9. Wang Z-B, and Xu J. 2020. Better Adjuvants for Better Vaccines: Progress in Adjuvant Delivery Systems, Modifications, and Adjuvant–Antigen Codelivery. Nato Adv Sci Inst Se 8: 128.
10. Fabrizi F, Cerutti R, Garcia-Agudo R, Bellincioni C, Porata G, Frontini G, Aoufi-Rabih S, and Messa P. 2020. Adjuvanted recombinant HBV vaccine (HBV-AS04) is effective over extended follow-up in dialysis population. An open-label non randomized trial. Clin Res Hepatol Gas 44: 905–912.
11. Skinner SR, Apter D, Carvalho ND, Harper DM, Konno R, Paavonen J, Romanowski B, Roteli-Martins C, Burlet N, Mihalyi A, and Struyf F. 2016. Human papillomavirus (HPV)-16/18 AS04-adjuvanted vaccine for the prevention of cervical cancer and HPV-related diseases. Expert Rev Vaccines 15: 367–387. [PubMed: 26902666]
12. Wang Y-Q, Bazin-Lee H, Evans JT, Casella CR, and Mitchell TC 2020. MPL Adjuvant Contains Competitive Antagonists of Human TLR4. Front Immunol 11: 577823.
13. Kolb JP, Casella CR, SenGupta S, Chilton PM, and Mitchell TC 2014. Type I interferon signaling contributes to the bias that Toll-like receptor 4 exhibits for signaling mediated by the adaptor protein TRIF. Sci Signal 7: ra108.
14. Tanimura N, Saitoh S, Ohto U, Akashi-Takamura S, Fujimoto Y, Fukase K, Shimizu T, and Miyake K. 2014. The attenuated inflammation of MPL is due to the lack of CD14-dependent tight dimerization of the TLR4/MD2 complex at the plasma membrane. Int Immunol 26: 307–314. [PubMed: 24380872]
15. Frederick DR, Goggins JA, Sabbagh LM, Freytag LC, Clements JD, and McLachlan JB 2018. Adjuvant selection regulates gut migration and phenotypic diversity of antigen-specific CD4+ T cells following parenteral immunization. Mucosal Immunol 11: 549–561. [PubMed: 28792004]
16. Brereton CF, Sutton CE, Ross PJ, Iwakura Y, Pizza M, Rappuoli R, Lavelle EC, and Mills KHG 2011. Escherichia coli Heat-Labile Enterotoxin Promotes Protective Th17 Responses against Infection by Driving Innate IL-1 and IL-23 Production. J Immunol 186: 5896–5906. [PubMed: 21490151]
17. Clements JD, and Norton EB 2018. The Mucosal Vaccine Adjuvant LT(R192G/L211A) or dmLT. Msphere 3: e00215–18.
18. Larena M, Holmgren J, Lebens M, Terrinoni M, and Lundgren A. 2015. Cholera Toxin, and the Related Nontoxic Adjuvants mmCT and dmLT, Promote Human Th17 Responses via Cyclic AMP–Protein Kinase A and Inflammasome-Dependent IL-1 Signaling. J Immunol 194: 3829–3839. [PubMed: 25786687]
19. Ryan EJ, McNeela E, Pizza M, Rappuoli R, O'Neill L, and Mills KHG 2000. Modulation of Innate and Acquired Immune Responses by Escherichia coli Heat-Labile Toxin: Distinct Pro- and Anti-Inflammatory Effects of the Nontoxic AB Complex and the Enzyme Activity. J Immunol 165: 5750–5759. [PubMed: 11067933]
20. Kelley N, Jeltema D, Duan Y, and He Y. 2019. The NLRP3 Inflammasome: An Overview of Mechanisms of Activation and Regulation. Int J Mol Sci 20: 3328. [PubMed: 31284572]
21. Rathinam VAK, and Fitzgerald KA 2016. Inflammasome Complexes: Emerging Mechanisms and Effector Functions. Cell 165: 792–800. [PubMed: 27153493]
22. Evavold CL, and Kagan JC 2019. Inflammasomes: Threat-Assessment Organelles of the Innate Immune System. Immunity 51: 609–624. [PubMed: 31473100]
23. Russo AJ, Vasudevan SO, Méndez-Huergo SP, Kumari P, Menoret A, Duduskar S, Wang C, Sáez JMP, Fettis MM, Li C, Liu R, Wanchoo A, Chandiran K, Ruan J, Vanaja SK, Bauer M, Sponholz C, Hudalla GA, Vella AT, Zhou B, Deshmukh SD, Rabinovich GA, and Rathinam VA 2021. Intracellular immune sensing promotes inflammation via gasdermin D–driven release of a lectin alarmin. Nat Immunol 22: 154–165. [PubMed: 33398185]
24. Evavold CL, Ruan J, Tan Y, Xia S, Wu H, and Kagan JC 2018. The Pore-Forming Protein Gasdermin D Regulates Interleukin-1 Secretion from Living Macrophages. Immunity 48: 35–44.e6.
25. Tsuchiya K, Hosojima S, Hara H, Kushiyama H, Mahib MR, Kinoshita T, and Suda T. 2021. Gasdermin D mediates the maturation and release of IL-1α downstream of inflammasomes. Cell Reports 34: 108887.

26. Patel S. 2017. Inflammasomes, the cardinal pathology mediators are activated by pathogens, allergens and mutagens: A critical review with focus on NLRP3. Biomed Pharmacother 92: 819–825. [PubMed: 28599247]
27. Norton EB, Lawson LB, Freytag LC, and Clements JD 2011. Characterization of a mutant Escherichia coli heat-labile toxin, LT(R192G/L211A), as a safe and effective oral adjuvant. Clin Vaccine Immunol Cvi 18: 546–51. [PubMed: 21288994]
28. Dobin A, Davis CA, Schlesinger F, Drenkow J, Zaleski C, Jha S, Batut P, Chaisson M, and Gingeras TR 2013. STAR: ultrafast universal RNA-seq aligner. Bioinformatics 29: 15–21. [PubMed: 23104886]
29. Kurtz JR, Nieves W, Bauer DL, Israel KE, Adcox HE, Gunn JS, Morici LA, and McLachlan JB 2020. Salmonella Persistence and Host Immunity Are Dictated by the Anatomical Microenvironment. Infect Immun 88.
30. Moon JJ, Chu HH, Pepper M, McSorley SJ, Jameson SC, Kedl RM, and Jenkins MK 2007. Naive CD4(+) T cell frequency varies for different epitopes and predicts repertoire diversity and response magnitude. Immunity 27: 203 213.
31. Jenkins MK, Chu HH, McLachlan JB, and Moon JJ 2010. On the composition of the preimmune repertoire of T cells specific for Peptide-major histocompatibility complex ligands. Annu Rev Immunol 28: 275 294.
32. Moon JJ, Chu HH, Hataye J, Pagán AJ, Pepper M, McLachlan JB, Zell T, and Jenkins MK 2009. Tracking epitope-specific T cells. Nat Protoc 4: 565 581.
33. Clements JD, and Norton EB 2018. The Mucosal Vaccine Adjuvant LT(R192G/L211A) or dmLT. Msphere 3: 546.
34. Malissen B, Tamoutounour S, and Henri S. 2014. The origins and functions of dendritic cells and macrophages in the skin. Nat Rev Immunol 14: 417–428. [PubMed: 24854591]
35. Kayagaki N, Wong MT, Stowe IB, Ramani SR, Gonzalez LC, Akashi-Takamura S, Miyake K, Zhang J, Lee WP, Muszyński A, Forsberg LS, Carlson RW, and Dixit VM 2013. Noncanonical Inflammasome Activation by Intracellular LPS Independent of TLR4. Science 341: 1246–1249. [PubMed: 23887873]
36. Tsai TF 2013. Fluad®-MF59®-Adjuvanted Influenza Vaccine in Older Adults. Infect Chemother 45: 159–174. [PubMed: 24265964]
37. HogenEsch H, O'Hagan DT, and Fox CB 2018. Optimizing the utilization of aluminum adjuvants in vaccines: you might just get what you want. Npj Vaccines 3: 51. [PubMed: 30323958]
38. Calabro S, Tortoli M, Baudner BC, Pacitto A, Cortese M, O'Hagan DT, Gregorio ED, Seubert A, and Wack A. 2011. Vaccine adjuvants alum and MF59 induce rapid recruitment of neutrophils and monocytes that participate in antigen transport to draining lymph nodes. Vaccine 29: 1812–1823. [PubMed: 21215831]
39. Seubert A, Monaci E, Pizza M, O'Hagan DT, and Wack A. 2008. The Adjuvants Aluminum Hydroxide and MF59 Induce Monocyte and Granulocyte Chemoattractants and Enhance Monocyte Differentiation toward Dendritic Cells. J Immunol 180: 5402–5412. [PubMed: 18390722]
40. Bode C, Zhao G, Steinhagen F, Kinjo T, and Klinman DM 2014. CpG DNA as a vaccine adjuvant. Expert Rev Vaccines 10: 499–511.
41. Lee G-H, and Lim S-G 2021. CpG-Adjuvanted Hepatitis B Vaccine (HEPLISAV-B®) Update. Expert Rev Vaccines 20: 1–9. [PubMed: 33434084]
42. Pulendran B, Arunachalam PS, and O'Hagan DT 2021. Emerging concepts in the science of vaccine adjuvants. Nat Rev Drug Discov 20: 454–475. [PubMed: 33824489]
43. Syed YY 2018. Recombinant Zoster Vaccine (Shingrix®): A Review in Herpes Zoster. Drug Aging 35: 1031–1040.
44. Ragupathi G, Gardner JR, Livingston PO, and Gin DY 2014. Natural and synthetic saponin adjuvant QS-21 for vaccines against cancer. Expert Rev Vaccines 10: 463–470.
45. Lacaille-Dubois M-A 2019. Updated insights into the mechanism of action and clinical profile of the immunoadjuvant QS-21: A review☆. Phytomedicine 60: 152905–152905.

46. Lavelle EC, McNeela E, Armstrong ME, Leavy O, Higgins SC, and Mills KHG 2003. Cholera Toxin Promotes the Induction of Regulatory T Cells Specific for Bystander Antigens by Modulating Dendritic Cell Activation. J Immunol 171: 2384–2392. [PubMed: 12928385]
47. Zasłona Z, Pålsson-McDermott EM, Menon D, Haneklaus M, Flis E, Prendeville H, Corcoran SE, Peters-Golden M, and O'Neill LAJ 2017. The Induction of Pro–IL-1β by Lipopolysaccharide Requires Endogenous Prostaglandin E 2 Production. J Immunol 198: 3558–3564. [PubMed: 28298525]
48. Rieser C, Böck G, Klocker H, Bartsch G, and Thurnher M. 1997. Prostaglandin E2 and Tumor Necrosis Factor α Cooperate to Activate Human Dendritic Cells: Synergistic Activation of Interleukin 12 Production. J Exp Medicine 186: 1603–1608.
49. Sokolowska M, Chen L-Y, Liu Y, Martinez-Anton A, Qi H-Y, Logun C, Alsaaty S, Park YH, Kastner DL, Chae JJ, and Shelhamer JH 2015. Prostaglandin E2 Inhibits NLRP3 Inflammasome Activation through EP4 Receptor and Intracellular Cyclic AMP in Human Macrophages. J Immunol 194: 5472–5487. [PubMed: 25917098]
50. Serezani CH, Ballinger MN, Aronoff DM, and Peters-Golden M. 2008. Cyclic AMP: master regulator of innate immune cell function. Am J Resp Cell Mol 39: 127–32.
51. Bagley KC, Abdelwahab SF, Tuskan RG, and Lewis GK 2006. Cholera toxin indirectly activates human monocyte-derived dendritic cells in vitro through the production of soluble factors, including prostaglandin E(2) and nitric oxide. Clin Vaccine Immunol Cvi 13: 106–15. [PubMed: 16426007]
52. Lee G-S, Subramanian N, Kim AI, Aksentijevich I, Goldbach-Mansky R, Sacks DB, Germain RN, Kastner DL, and Chae JJ 2012. The calcium-sensing receptor regulates the NLRP3 inflammasome through Ca2+ and cAMP. Nature 492: 123–127. [PubMed: 23143333]
53. Chang D, Whiteley AT, Gwilt KB, Lencer WI, Mekalanos JJ, and Thiagarajah JR 2020. Extracellular cyclic dinucleotides induce polarized responses in barrier epithelial cells by adenosine signaling. P Natl Acad Sci Usa 117: 27502–27508.
54. Ko MK, Shao H, Kaplan HJ, and Sun D. 2020. CD73+ Dendritic Cells in Cascading Th17 Responses of Experimental Autoimmune Uveitis-Induced Mice. Front Immunol 11: 601272.
55. Boucher D, Monteleone M, Coll RC, Chen KW, Ross CM, Teo JL, Gomez GA, Holley CL, Bierschenk D, Stacey KJ, Yap AS, Bezbradica JS, and Schroder K. 2018. Caspase-1 self-cleavage is an intrinsic mechanism to terminate inflammasome activity. J Exp Medicine 215: 827–840.
56. Monteleone M, Stanley AC, Chen KW, Brown DL, Bezbradica JS, von Pein JB, Holley CL, Boucher D, Shakespear MR, Kapetanovic R, Rolfes V, Sweet MJ, Stow JL, and Schroder K. 2018. Interleukin-1β Maturation Triggers Its Relocation to the Plasma Membrane for Gasdermin-D-Dependent and -Independent Secretion. Cell Reports 24: 1425–1433. [PubMed: 30089254]
57. Zanoni I, Tan Y, Gioia MD, Springstead JR, and Kagan JC 2017. By Capturing Inflammatory Lipids Released from Dying Cells, the Receptor CD14 Induces Inflammasome-Dependent Phagocyte Hyperactivation. Immunity 47: 697–709.e3.
58. Zanoni I, Tan Y, Gioia MD, Broggi A, Ruan J, Shi J, Donado CA, Shao F, Wu H, Springstead JR, and Kagan JC 2016. An endogenous caspase-11 ligand elicits interleukin-1 release from living dendritic cells. Science 352: 1232 1236.
59. Zhivaki D, Borriello F, Chow OA, Doran B, Fleming I, Theisen DJ, Pallis P, Shalek AK, Sokol CL, Zanoni I, and Kagan JC 2020. Inflammasomes within Hyperactive Murine Dendritic Cells Stimulate Long-Lived T Cell-Mediated Anti-tumor Immunity. Cell Reports 33: 108381–108381.
60. Liu X, Xia S, Zhang Z, Wu H, and Lieberman J. 2021. Channelling inflammation: gasdermins in physiology and disease. Nat Rev Drug Discov 20: 384–405. [PubMed: 33692549]
61. Scandella E, Men Y, Gillessen S, Förster R, and Groettrup M. 2002. Prostaglandin E2 is a key factor for CCR7 surface expression and migration of monocyte-derived dendritic cells. Blood 100: 1354–1361. [PubMed: 12149218]
62. Zhivaki D, Borriello F, Chow OA, Doran B, Fleming I, Theisen DJ, Pallis P, Shalek AK, Sokol CL, Zanoni I, and Kagan JC 2020. Inflammasomes within Hyperactive Murine Dendritic Cells Stimulate Long-Lived T Cell-Mediated Anti- tumor Immunity. Cell Reports 33: 108381–108381.

Key Points:

- The adjuvant combination of dmLT and MPL-A can induce significant T cell expansion
- The adjuvant combination activates the NLRP3 inflammasome in dendritic cells
- Combination adjuvant IL-1β release from dendritic cells is gasdermin D independent

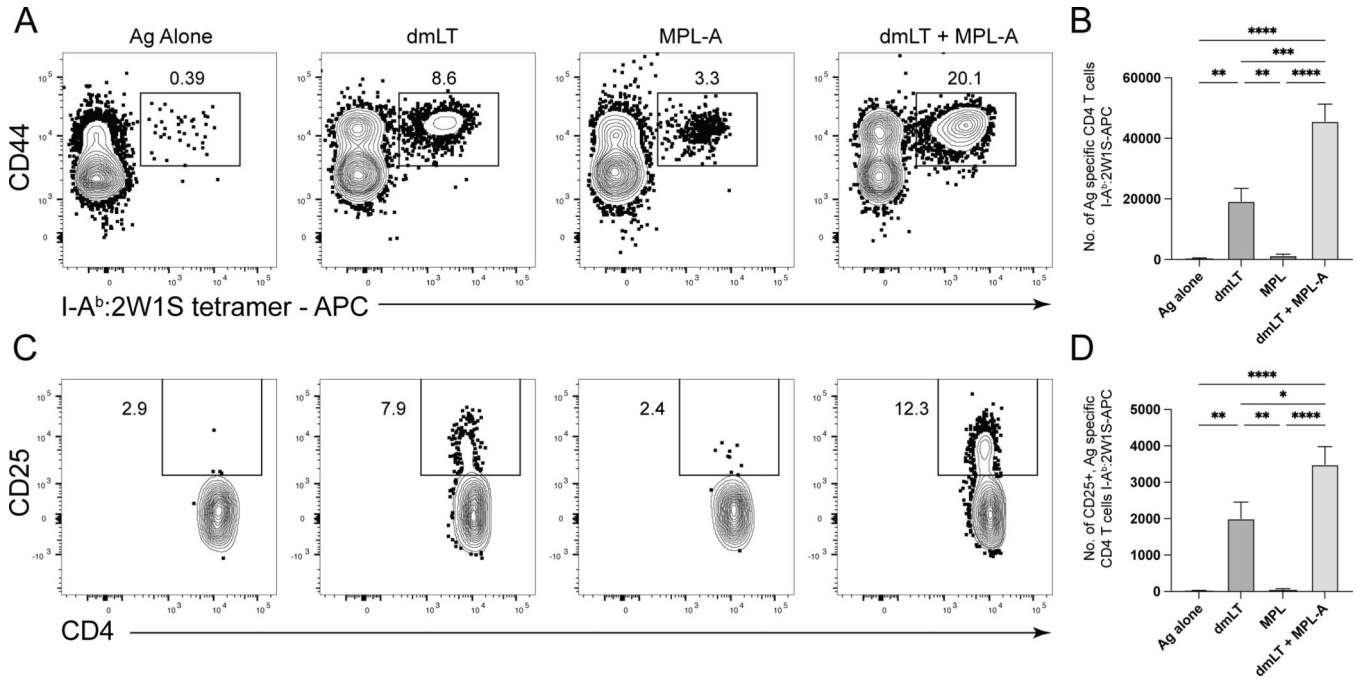

Figure 1. The combination adjuvant increases the expansion and activation of antigen-specific CD4 T cells during vaccination.

Mice were immunized intradermally with a single dose of the model antigen 2W1S with and without dmLT, MPL-A, or the combination of the two. 10 days later, the cervical lymph nodes were harvested and antigen-specific CD4 T cell responses were assessed by flow cytometry using MHC-II tetramers. (A, C) Representative flow plots from the CLN and total number of expanded (B) $CD44^+$ $I\text{-}A^b{:}2W1S^+$ CD4 T cells and (D) activated $CD25^+$ antigen-specific CD4 T cells were determined. Treatments were compared using One-Way ANOVA with Tukey's post hoc test for multiple comparisons (n=6 per group *, $p<0.05$; **, $p<0.01$; ***, $p<0.001$; ****$p<0.0001$). Data shows a representation of 4 independent experiments. Numbers above gates represent the (A) percent of antigen specific CD4 T cells out of CD4 T cells and the (C) percent of antigen specific CD4 T cells expressing CD25.

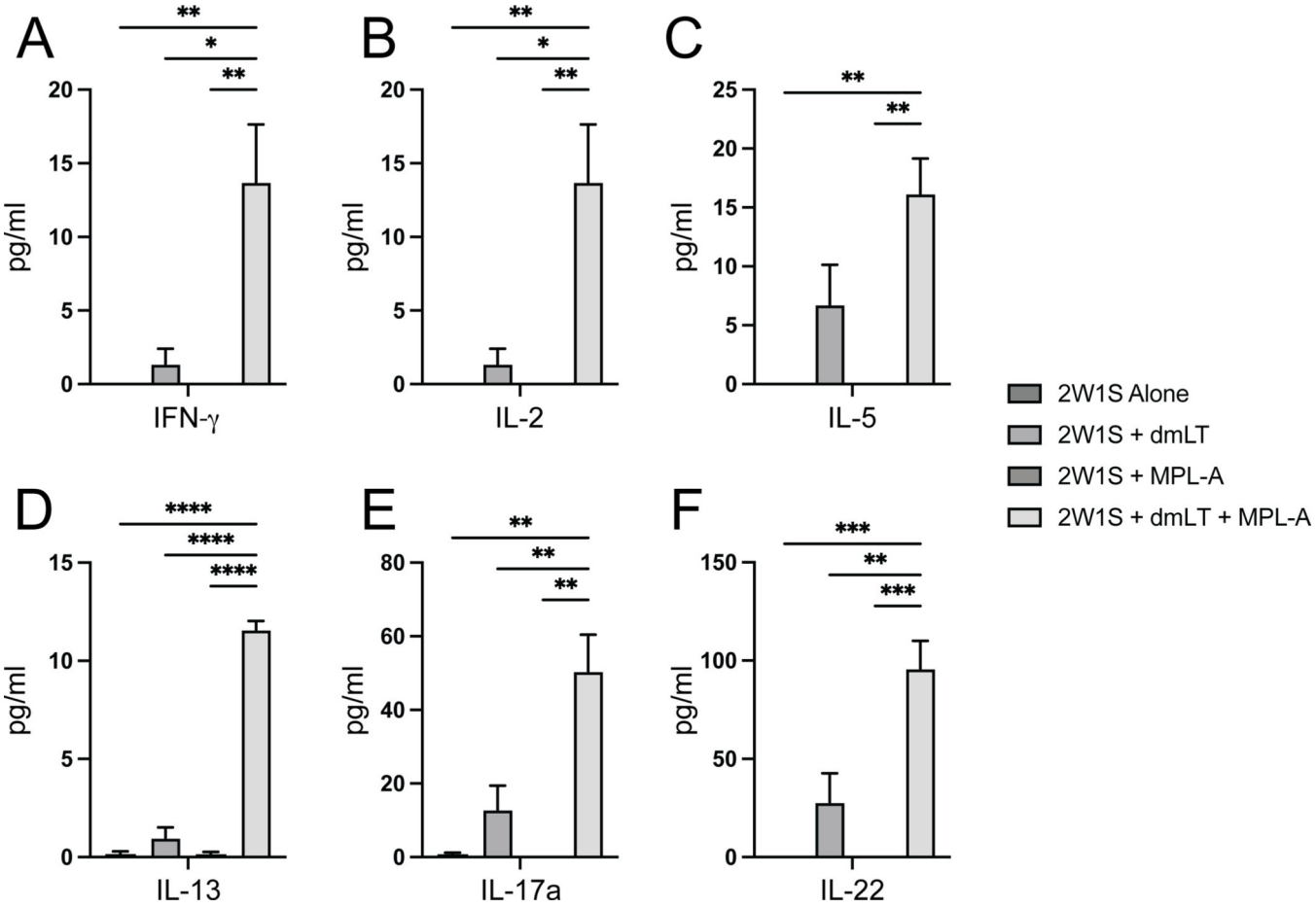

Figure 2. The combination adjuvant imparts a mixed Th phenotype in antigen specific CD4 T cells following vaccination.

Mice were immunized intradermally in the ear with the model antigen 2W1S with and without dmLT, MPL-A, or the combination of the two. 10 days later, the cervical lymph nodes were harvested, and antigen-specific CD4 T cells were enriched using MHC-II tetramers and column-based magnetic cell isolation. Enriched 2W1S cells were counted, plated in a 96-well plate at 1×10^6 cells/well, and stimulated with 2W1S antigen for 72 hours at 37C, 5% CO2. Cell supernatants were harvested, and secreted cytokines were assessed. Treatments were compared using One-Way ANOVA with Tukey's post hoc test for multiple comparisons (n=3 per group *, $p<0.05$; **, $p<0.01$; ***, $p<0.001$; ****$p<0.0001$). Data show a representation of 2 independent experiments.

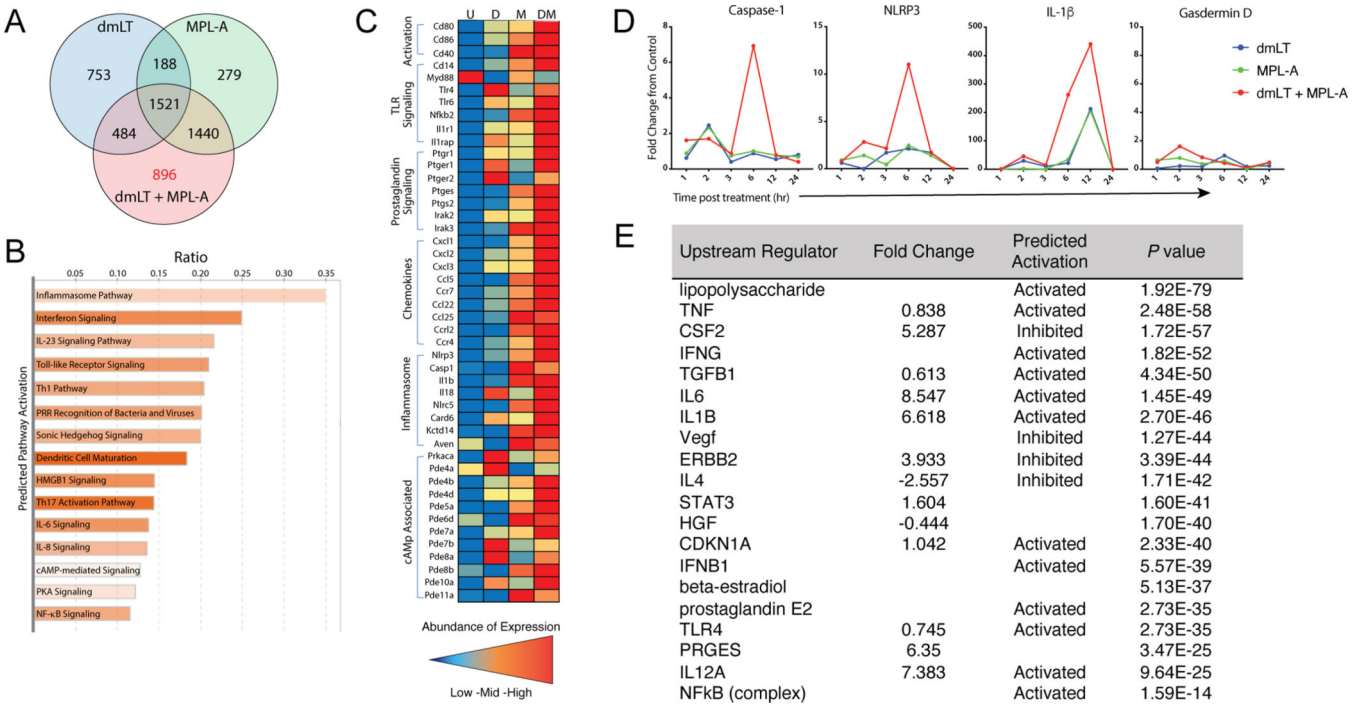

Upstream Regulator	Fold Change	Predicted Activation	*P* value
lipopolysaccharide		Activated	1.92E-79
TNF	0.838	Activated	2.48E-58
CSF2	5.287	Inhibited	1.72E-57
IFNG		Activated	1.82E-52
TGFB1	0.613	Activated	4.34E-50
IL6	8.547	Activated	1.45E-49
IL1B	6.618	Activated	2.70E-46
Vegf		Inhibited	1.27E-44
ERBB2	3.933	Inhibited	3.39E-44
IL4	-2.557	Inhibited	1.71E-42
STAT3	1.604		1.60E-41
HGF	-0.444		1.70E-40
CDKN1A	1.042	Activated	2.33E-40
IFNB1		Activated	5.57E-39
beta-estradiol			5.13E-37
prostaglandin E2		Activated	2.73E-35
TLR4	0.745	Activated	2.73E-35
PRGES	6.35		3.47E-25
IL12A	7.383	Activated	9.64E-25
NFkB (complex)		Activated	1.59E-14

Figure 3. The combination adjuvant distinctly alters the transcription profile in DCs with an enrichment in canonical inflammasome signaling.

BMDCs were cultured from the bone marrow of C57BL/6 mice. Cells were seeded in 6 well plates at a concentration of 1×10^6 cells/mL and stimulated with dmLT (D), MPL-A (M), or a combination (DM) for 24 hours. Cells were centrifuged, RNA extracted, and paired-end mRNA sequencing was performed. (A) Comparative analysis of differentially expressed genes between each treatment and (B) shows the pathway analysis of the top predicted upregulated pathways in the combination adjuvant treated BMDCs. The resulting biological functions, canonical pathways, and upstream regulators were filtered by setting a threshold of $P < 0.05$ using Fisher's exact test. (C) Selected gene expression profiles show the abundance of expression relative to untreated and (D) cDNA was also generated and RT-qPCR was performed in a time course on select inflammasome genes. (E) Analysis of predicted upstream regulators from RNA sequence data was performed using IPA software. Data was analyzed using the ΔΔCT method, normalizing all samples to GAPDH and comparing relative expression levels to those of untreated cells. Treatments were compared using Two-Way ANOVA with Dunnett's post hoc test for multiple comparisons (n=3 per treatment per timepoint *, $p<0.05$; **, $p<0.01$; ***, $p<0.001$; ****$p<0.0001$). Data show a representation of 2 independent experiments.

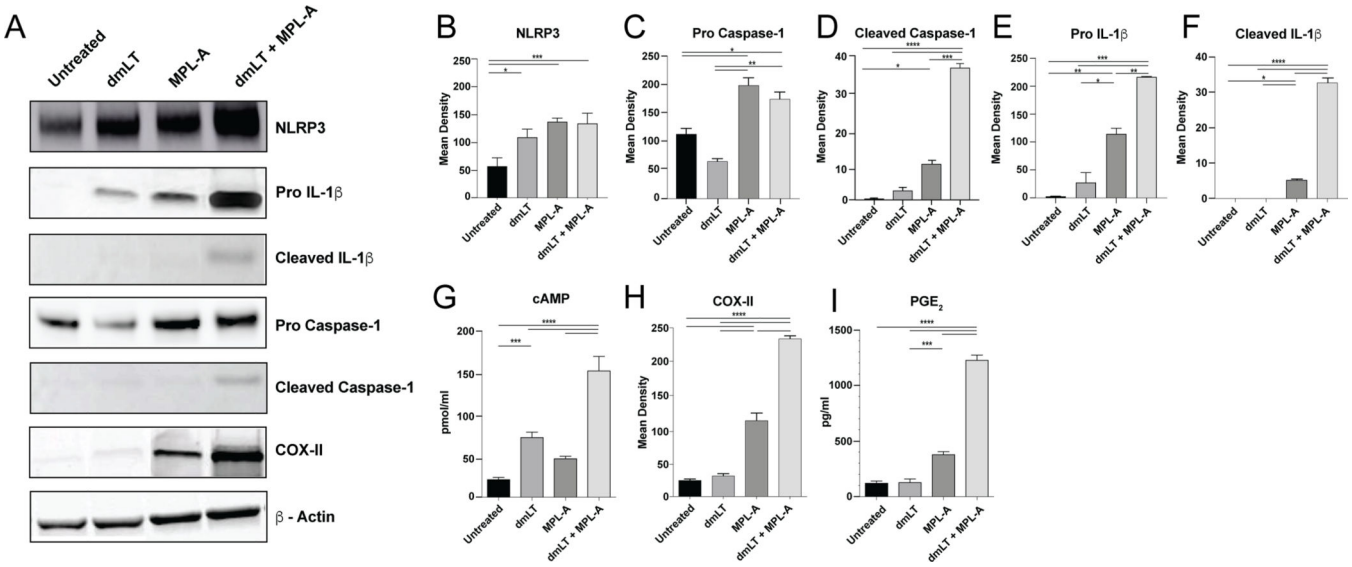

Figure 4. The combination adjuvant activates the NLRP3 inflammasome and increases the production of secondary messengers.

BMDCs were cultured from the bone marrow of C57BL/6 mice. Cells were seeded in 6 well plates at a concentration of 1×10^6 cells/ml and stimulated with dmLT, MPL, or in combination for 24 hours at 37C. BMDCs were lysed and assessed via western blot (A-F) to determine cytosolic NLRP3, pro and cleaved IL-1β and caspase 1, (H) COX-II, and β-actin as a standardization control and (I) supernatant was assayed for PGE_2 by ELISA. (G) After 21 hours, the phosphodiesterase (PDE) inhibitors rolipram and cilostazol were added at 50μM to prevent conversion of the secondary messenger cAMP and cell lysates and supernatant harvested at 24 hours to determine total cAMP induction. Treatments were compared using One-Way ANOVA with Tukey's post hoc test for multiple comparisons (n=3 per treatment *, $p<0.05$; **, $p<0.01$; ***, $p<0.001$; ****$p<0.0001$). Data show a representation of 3 independent experiments.

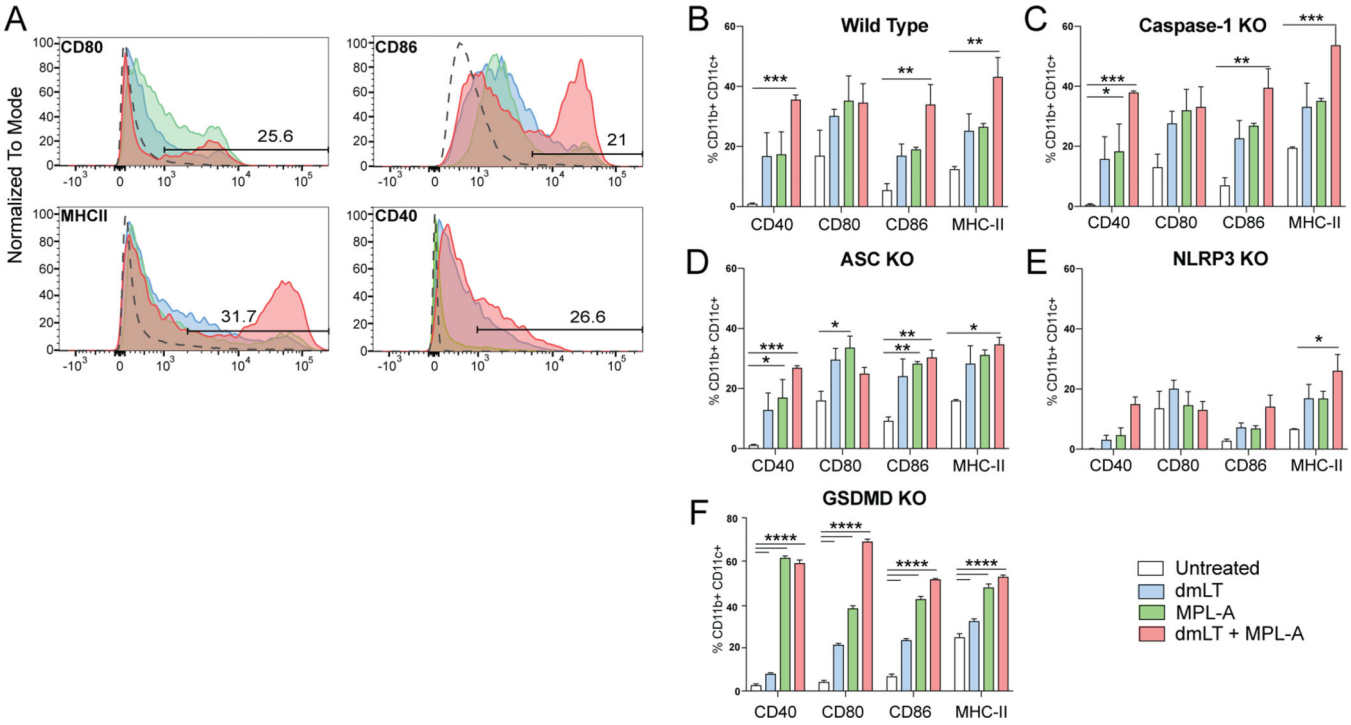

Figure 5. Activation of DCs is NLRP3 dependent, but Caspase 1 and GSDMD independent.

BMDCs were cultured from the bone marrow of wild type, NLRP3 KO, ASC KO, Caspase 1 KO, and GSDMD KO mice. Cells were seeded in 6 well plates at a concentration of 1×10^6 cells/mL and were left untreated or stimulated with dmLT, MPL, or a combination of the two for 24 hours. Cells were analyzed for the expression of surface markers indicative of activation by flow cytometry. (A) Representative gating strategy for the expression of activation markers CD40, CD80, CD86, and MHC-II in cells differentiated from wild type animals. Data show the percentage of DCs positive for each activation marker in (B) wild type, (C) Caspase 1 KO, (D) ASC KO, (E) NLRP3 KO, and (F) GSDMD KO cells. Treatments were compared using Two-Way ANOVA with Tukey's post hoc test for multiple comparisons (n=3 per treatment per timepoint *, $p<0.05$; **, $p<0.01$; ***, $p<0.001$; ****$p<0.0001$). Data show a representation of 3 independent experiments.

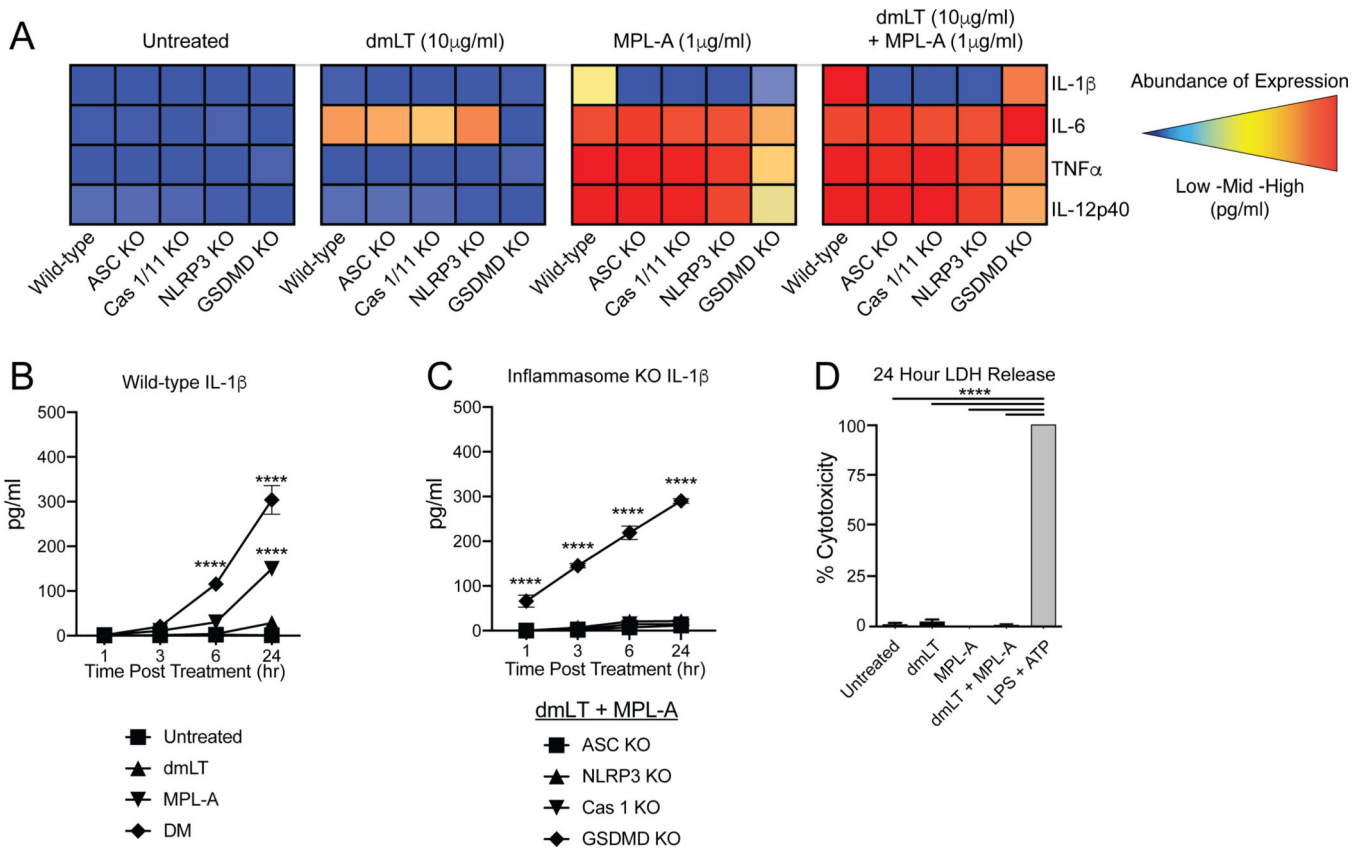

Figure 6. IL-1β secretion, but not other Th polarizing cytokines require key components of the NLRP3 inflammasome complex but are independent of gasdermin D mediated pyroptosis.

BMDCs were cultured from the bone marrow of wild type and inflammasome KO C57BL/6 background mouse femurs and differentiated using GM-CSF. Cells were seeded in 96 well plates at a concentration of 1.5×10^5 cells per well and stimulated with dmLT MPL-A, or a combination of the two for 1, 3, 6 and 24 hours. (A) heat maps IL-1β, IL-6, TNF, and IL-12p40 secretion after 24 hours is shown (B) IL-1β kinetics from single and combination adjuvant treated wild type and (C) combination adjuvant treated inflammasome KO BMDCs was determined via ELISA and expressed as pg/ml. (D) Cytotoxicity was determined after 24 hours by quantifying LDH release with LPS + ATP treatment serving as a positive control. Significance was calculated using two-way ANOVA with Dunnetts post hoc test for multiple comparisons against untreated (A), GSDMD (B), and LPS + ATP (C) (n=3–6 per group ****, $p < 0.0001$). Data shown is a representation of 3 independent experiments.

Table 1.

Interactions tested for effects greater than those explained by dmLT or MPL-A alone.

Outcome	dmLT:MPL-A interaction*	p-value
Number cells (SD)		
CLN	25309 (7069)	0.002
Secreted cytokines CLN, pg/ml (SD)		
IFN-γ	12.4 (4.1)	0.02
IL-13	10.6 (0.7)	<0.001
IL-17A	38.4 (11.9)	0.01
IL-22	67.9 (2.0)	0.01
Secreted cytokines BMDC 24 hours, pg/ml (SD)		
PGE_2	840.5 (63.0)	< 0.001
IL-1β	124.7 (5.5)	< 0.001

*Interaction effects are the amount greater than the additive effects of dmLT or MPL-A alone with p-values indicating if these effects were found to be significantly non-zero (greater than the sum of the effects of dmLT and MPL-A) found by linear regression for each indicated outcome.

Abbreviations: CLN, cervical lymph node; dmLT, double mutant heat-labile toxin; IFN, interferon; IL, interleukin; MPL-A monophosphoryl lipid A; PGE2 Prostaglandin E2